Waveform and Passive Beamforming Design for Intelligent Reflecting Surface-Aided Wireless Information and Power Transfer

Yang Zhao

Department of Electrical and Electronic Engineering
Imperial College London

Early Stage Assessment, July 3, 2020

Table of Contents

What is WPT?

Wireless Power Transfer (WPT) varies electromagnetic fields to deliver power.

Table: WPT Technologies

Categories	Technology	Devices	Power	Frequency	Range
Near-field	Magnetic resonant coupling	Resonators	Up to 10 W	kHz – MHz	m
	Inductive coupling	Wire coils	Up to 10 W	Hz – MHz	mm – cm
	Capacitive coupling	Metal plates	Up to 1 W	kHz – MHz	mm
Far-field	RF waves	Rectennas	μW – mW	MHz – GHz	m – km
	Light waves	Lasers	μW – mW	THz	km

Characteristics:

- no wires and batteries
- everlasting, controllable, reliable, sustainable

WPT by RF waves

Energy flow: DC → RF → RF → DC

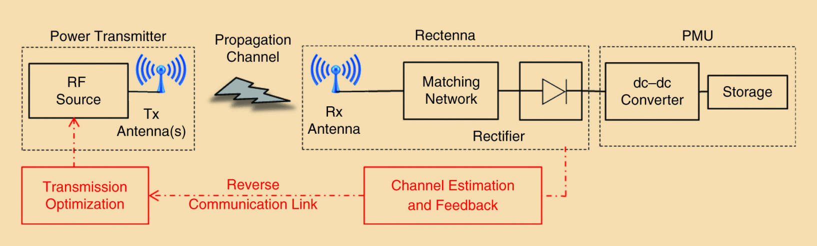

Pros:

- long range (up to hundreds of m) with NLoS support
- compact receiver (few cm), easy integration
- suitable for mobile devices

Cons:

- low power level (μW – mW)
- low energy harvesting efficiency (40% at 100 μW, 20% at 10 μW)

Figure from [1]

Why RF waves?

RF waves enables:

- Wireless communication (WIT)
- WPT

Simultaneous Wireless Information and Power Transfer (SWIPT): downlink WIT and WPT at the same time. Receivers can be either separated or co-located.

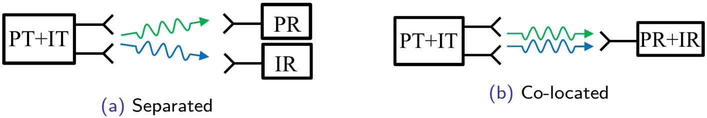

Figure: SWIPT receivers

Figure from [2]

Co-located receiver architecture

Two practical receiver architecture:

- **Time-Switching** (TS) switches between Information Decoding (ID) and Energy Harvesting (EH) modes on time basis.
- **Power-Splitting** (PS) splits the received signal into individual components for ID and EH.

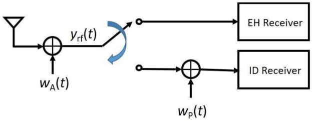

(a) TS

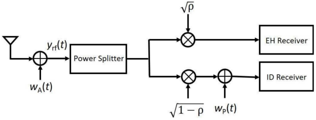

(b) PS

Figure: Co-located receiver architecture

Design issue

- TS can be achieved by a time sharing between WIT and WPT. Waveform is optimized individually for both cases.
- In PS, the splitting ratio ρ is coupled with the waveform design.

Harvester model

RF-to-DC conversion requires **rectenna** (receive antenna + rectifier), whose behavior is dominated by diode I-V characteristics.

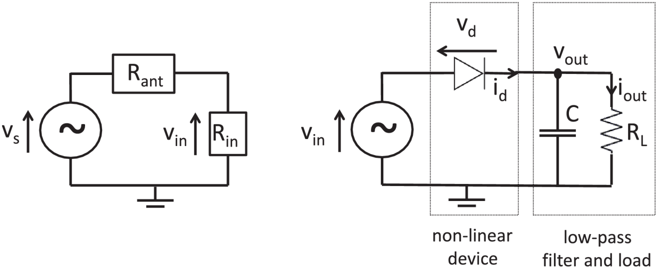

Figure: Rectenna equivalent circuit and a single diode rectifier [1]

Consider small-signal model and truncate its Taylor expansion to the n_0-th order:

- diode linear model ($n_o = 2$): output power is proportional to input power
- diode nonlinear model ($n_o > 2$): contribution from high-order terms

Figure from [2]

Waveform design

A superposed signal containing modulated information waveform and multisine power waveform is demonstrated to bring a two-fold benefit:

- **rate**: multisine is deterministic with no interference on information waveform (by waveform cancellation or translated codebook)
- **energy**: multisine brings high PAPR and triggers the diode nonlinear model more often (reduce threshold from -20 dBm to -30 dBm)

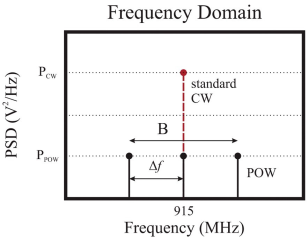

(a) Frequency domain

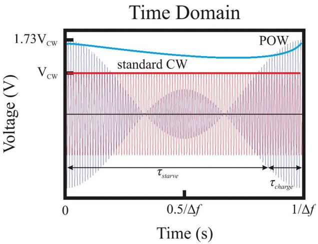

(b) Time domain

Figure: Multisine waveform

Figure from [3]

What is IRS?

Intelligent Reflecting Surface (IRS) consists of multiple individual passive reflecting elements that adjust the amplitude and phase of the incident signal.

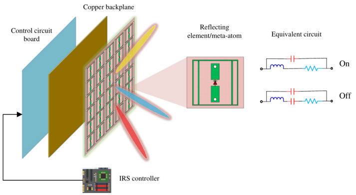

(a) IRS architecture

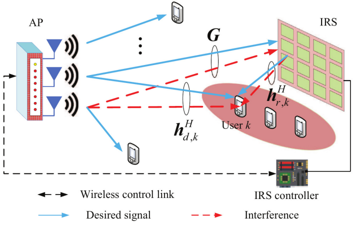

(b) Application scenario

- outer layer: redistribute incident signals
- middle layer: avoid signal energy leakage
- inner layer: adjust reflection amplitude and phase shift

- enhance primary transmission by constructive reflection
- null interference by destructive reflection

Figure from [4, 5]

Why IRS?

Characteristics:

- passive (different from AF relay)
    - no RF chains
    - low power consumption
    - no additional thermal noise
    - squared gain: received power scales quadratically with the number of reflectors (boost receive power and array gain in equal gain transmission)
- full-duplex
- assistant (different from backscatter node)
- adjustable in real-time

Challenges:

- channel estimation
    - cannot separate incident and reflective channels
    - large number of extra channels
- practical restriction
    - discrete phase shifts
    - phase shift are coupled with reflection amplitude (by impedance equation)

Why IRS-aided SWIPT?

- both aim at improving spectral/energy efficiency
- enhanced channel boosts received power to benefit from harvester nonlinearity
- extra links increase system diversity and stability, which is essential for SWIPT
- SWIPT can potentially support low-power IRS

Approaches

Separated information decoder and energy harvester:

- [6] investigated a MISO system with energy interference and proved at most one energy beam is required to maximize the WSP subject to SINR constraints.
- [7] considered fairness issue for a MISO system and maximized the minimum output power based on perfect energy interference cancellation.
- [8] transformed WSR maximization of MIMO SWIPT to WMMSE problem then solved by BCD with low-complexity iterative algorithms.
- [9] proposed a penalty-based algorithm to minimize transmit power of MISO system subject to SINR constraints, whose inner layer updates precoders, phase shifts and auxiliary variables by BCD while the outer layer updates the penalty coefficients.

Outcomes and opportunities

Outcomes:

- IRS brings a significant gain to SWIPT
- performance vary significantly under different configuration (distances, number of reflectors, transmit power, SNR, etc)
- dedicated energy beam is necessary to boost the harvested power
- LoS links can further increase the harvested power, since rank-deficient channels are highly correlated and a single energy stream can provide large output power for multiple harvesters

Opportunities:

- no works on co-located information decoder and energy harvester
- no works on IRS-aided OFDM SWIPT
- no works consider harvester nonlinearity
- no works investigate Rate-Energy (R-E) tradeoff

Table of Contents

Signal and channel

SISO, L-reflector IRS, K-user, N-subband

- transmit signal at the AP:

$$x(t) = \Re\left\{\sum_{n=1}^{N} \left(w_{I,n}\tilde{x}_{I,n}(t) + w_{P,n}\right) e^{j2\pi f_n t}\right\} \tag{1}$$

  - $w_{I/P,n}$ collects magnitude and phase of the information and power signal
  - $\tilde{x}_{I,n} \sim \mathcal{CN}(0,1)$ is the information symbol
- composite channel for user k:
  - direct: AP-user ($h_{D,k,n}$)
  - extra: AP-IRS ($\boldsymbol{h}_{I,n}$), IRS reflection ($\boldsymbol{\Theta}$), IRS-user ($\boldsymbol{h}_{R,k,n}^H$)

$$h_{E,k,n} = \boldsymbol{h}_{R,k,n}^H \boldsymbol{\Theta} \boldsymbol{h}_{I,n} = \boldsymbol{v}_{k,n}^H \boldsymbol{\phi} \tag{2}$$

  - sum up and stack over all subbands:

$$\boldsymbol{h}_k = \boldsymbol{h}_{D,k} + \boldsymbol{V}_k^H \boldsymbol{\phi} \tag{3}$$

- received signal by user k

$$y_k(t) = \Re\left\{\sum_{n=1}^{N} h_{k,n}\left(w_{I,n}\tilde{x}_{I,n}(t) + w_{P,n}\right) e^{j2\pi f_n t}\right\} \tag{4}$$

Information decoder

The power component $y_{P,k}(t)$ creates no interference to the information component $y_{I,k}(t)$. Hence, the achievable rate of user k is

$$R_k(\boldsymbol{w}_I, \phi, \rho, \boldsymbol{\alpha}_k) = \sum_{n=1}^{N} \alpha_{k,n} \log_2 \left(1 + \frac{(1-\rho)|h_{k,n} w_{I,n}|^2}{\sigma_n^2}\right) \tag{5}$$

- ρ is the splitting ratio for energy harvesting
- $\alpha_{k,n}$ is the allocation indicator:

$$\alpha_{k,n} = \begin{cases} 1, & \text{if subband } n \text{ is given to user } k \\ 0, & \text{otherwise} \end{cases} \tag{6}$$

- σ_n^2 is the variance of the noise at RF band and during RF-to-BB conversion

Energy harvester

A **truncated Taylor expansion** of small signal model highlights the dependency of harvester output DC current on the received waveform:

$$z_k(\boldsymbol{w}_I, \boldsymbol{w}_P, \phi, \rho) = \sum_{i \text{ even}, i \geq 2}^{n_0} k_i \rho^{i/2} R_{\text{ant}}^{i/2} \mathcal{E}\left\{\mathcal{A}\left\{y_k(t)^i\right\}\right\} \tag{7}$$

Pick $n_0 = 4$ and we have:

$$\begin{aligned}
z_k(\boldsymbol{w}_I, \boldsymbol{w}_P, \phi, \rho) &= \beta_2\rho\left(\mathcal{E}\left\{\mathcal{A}\left\{y_{I,k}^2(t)\right\}\right\} + \mathcal{A}\left\{y_{P,k}^2(t)\right\}\right) + \beta_4\rho^2\left(\mathcal{E}\left\{\mathcal{A}\left\{y_{I,k}^4(t)\right\}\right\} + \mathcal{A}\left\{y_{P,k}^4(t)\right\} + 6\mathcal{E}\left\{\mathcal{A}\left\{y_{I,k}^2(t)\right\}\right\}\mathcal{A}\left\{y_{P,k}^2(t)\right\}\right) \\
&= \frac{1}{2}\beta_2\rho(\boldsymbol{h}_k^H \boldsymbol{W}_{I,0}\boldsymbol{h}_k + \boldsymbol{h}_k^H \boldsymbol{W}_{P,0}\boldsymbol{h}_k) \\
&\quad + \frac{3}{8}\beta_4\rho^2\left(2(\boldsymbol{h}_k^H \boldsymbol{W}_{I,0}\boldsymbol{h}_k)^2 + \sum_{n=-N+1}^{N-1}(\boldsymbol{h}_k^H \boldsymbol{W}_{P,n}^*\boldsymbol{h}_k)(\boldsymbol{h}_k^H \boldsymbol{W}_{P,n}^*\boldsymbol{h}_k)^*\right) \\
&\quad + \frac{3}{2}\beta_4\rho^2(\boldsymbol{h}_k^H \boldsymbol{W}_{I,0}\boldsymbol{h}_k)(\boldsymbol{h}_k^H \boldsymbol{W}_{P,0}\boldsymbol{h}_k) \\
&= \frac{1}{2}\beta_2\rho(\boldsymbol{w}_I^H \boldsymbol{H}_{k,0}\boldsymbol{w}_I + \boldsymbol{w}_P^H \boldsymbol{H}_{k,0}\boldsymbol{w}_P) \\
&\quad + \frac{3}{8}\beta_4\rho^2\left(2(\boldsymbol{w}_I^H \boldsymbol{H}_{k,0}\boldsymbol{w}_I)^2 + \sum_{n=-N+1}^{N-1}(\boldsymbol{w}_P^H \boldsymbol{H}_{k,n}^*\boldsymbol{w}_P)(\boldsymbol{w}_P^H \boldsymbol{H}_{k,n}^*\boldsymbol{w}_P)^*\right) \\
&\quad + \frac{3}{2}\beta_4\rho^2(\boldsymbol{w}_I^H \boldsymbol{H}_{k,0}\boldsymbol{w}_I)(\boldsymbol{w}_P^H \boldsymbol{H}_{k,0}\boldsymbol{w}_P)
\end{aligned}$$

Rate-energy region

Define the achievable weighted sum **R-E region** as

$$C_{R-I}(P) \triangleq \left\{ (R, Z) : R \leq \sum_{k=1}^{K} u_{I,k} R_k, \, Z \leq \sum_{k=1}^{K} u_{P,k} z_k, \right. \\ \left. \frac{1}{2}(\boldsymbol{w}_I^H \boldsymbol{w}_I + \boldsymbol{w}_P^H \boldsymbol{w}_P) \leq P \right\} \tag{8}$$

- P is the transmit power budget
- $u_{I/P,k}$ are the information and power weight of user k

Table of Contents

Problem formulation

We characterize the rate-energy region through a current maximization problem subject to transmit power, rate, and IRS constraints

$$\max_{\boldsymbol{w}_I, \boldsymbol{w}_P, \boldsymbol{\phi}, \rho} \quad z(\boldsymbol{w}_I, \boldsymbol{w}_P, \boldsymbol{\phi}, \rho) \tag{9a}$$

$$\text{s.t.} \quad \frac{1}{2}(\boldsymbol{w}_I^H \boldsymbol{w}_I + \boldsymbol{w}_P^H \boldsymbol{w}_P) \leq P, \tag{9b}$$

$$\sum_n \log_2 \left(1 + \frac{(1-\rho)|(h_{D,n} + \boldsymbol{v}_n^H \boldsymbol{\phi}) w_{I,n}|^2}{\sigma_n^2}\right) \geq \bar{R}, \tag{9c}$$

$$|\phi_l| = 1, \quad l = 1, \ldots, L, \tag{9d}$$

$$0 \leq \rho \leq 1 \tag{9e}$$

$\boldsymbol{w}_{I/P}, \boldsymbol{\phi}, \rho$ are coupled in 9a, 9c, consider **alternating optimization** (AO).

Frequency-selective IRS

The ideal **Frequency-Selective** (FS) IRS provides:

- subband-dependent reflection coefficients (ϕ_n replaces ϕ)
- total DoF NL

Note that $|(h_{D,n} + \boldsymbol{v}_n^H \phi_n) w_{I,n}| \leq |h_{D,n} w_{I,n}| + |\boldsymbol{v}_n^H \phi_n w_{I,n}|$ and the equality holds when the direct and IRS-aided links are aligned. Therefore, we simply select the phase shift of element l at subband n as

$$\theta_{n,l}^{\star} = \angle h_{D,n} - \angle h_{R,n,l} - \angle h_{I,n,l} \tag{10}$$

That is to say, the optimal phase shift for FS-IRS is obtained in closed form in the single-user scenario, which ensures the direct, extra and composite channels have the same phase.

Frequency-flat IRS (1)

Frequency-Flat (FF) IRS reflects all subbands equally with a DoF of L.

Semi-Definite Relaxation (SDR): rate constraint

To simplify rate constraint 9c, we observe that

$$\begin{aligned} |h_{D,n} + \boldsymbol{v}_n^H \phi|^2 &= |h_{D,n}|^2 + h_{D,n}^* \boldsymbol{v}_n^H \phi + \phi^H \boldsymbol{v}_n h_{D,n} + \phi^H \boldsymbol{v}\boldsymbol{v}^H \phi \\ &= \bar{\phi}^H \boldsymbol{R}_n \bar{\phi} = \mathrm{Tr}(\boldsymbol{R}_n \bar{\phi}\bar{\phi}^H) = \mathrm{Tr}(\boldsymbol{R}_n \boldsymbol{\Phi}) \end{aligned} \tag{11}$$

where t is an auxiliary variable with unit modulus and

$$\boldsymbol{R}_n = \begin{bmatrix} \boldsymbol{v}_n \boldsymbol{v}_n^H & \boldsymbol{v}_n h_{D,n} \\ h_{D,n}^* \boldsymbol{v}_n^H & h_{D,n}^* h_{D,n} \end{bmatrix}, \quad \bar{\phi} = \begin{bmatrix} \phi \\ t \end{bmatrix}, \quad \boldsymbol{\Phi} = \bar{\phi}\bar{\phi}^H \tag{12}$$

Frequency-flat IRS (2)

We optimize $\boldsymbol{\Phi}$ with given waveform $\boldsymbol{w}_{I/P}$ and splitting ratio ρ.

SDR: current expression

Define $\boldsymbol{M} = [\boldsymbol{V}^H, \boldsymbol{h}_D]^H$ such that $\boldsymbol{h}\boldsymbol{h}^H = \boldsymbol{M}^H \boldsymbol{\Phi} \boldsymbol{M}$. Introduce auxiliary variables

$$\begin{aligned} t_{I/P,n} &= \boldsymbol{h}^H \boldsymbol{W}_{I/P,n}^* \boldsymbol{h} = \mathrm{Tr}(\boldsymbol{h}\boldsymbol{h}^H \boldsymbol{W}_{I/P,n}^*) = \mathrm{Tr}(\boldsymbol{M}^H \boldsymbol{\Phi} \boldsymbol{M} \boldsymbol{W}_{I/P,n}^*) \\ &= \mathrm{Tr}(\boldsymbol{M} \boldsymbol{W}_{I/P,n}^* \boldsymbol{M}^H \boldsymbol{\Phi}) = \mathrm{Tr}(\boldsymbol{C}_{I/P,n} \boldsymbol{\Phi}) \end{aligned} \tag{13}$$

Therefore, the current expression rewrites as

$$z(\boldsymbol{\Phi}) = \frac{1}{2}\beta_2 \rho (t_{I,0} + t_{P,0}) + \frac{3}{8}\beta_4 \rho^2 \left(2t_{I,0}^2 + \sum_{n=-N+1}^{N-1} t_{P,n} t_{P,n}^* \right) + \frac{3}{2}\beta_4 \rho^2 t_{I,0} t_{P,0} \tag{14}$$

Frequency-flat IRS (3)

We use first-order Taylor expansion to approximate the second-order terms in 14. Based on the variables optimized at iteration $i-1$, the local approximation at iteration i gives

$$(t_{I,0}^{(i)})^2 \geq 2t_{I,0}^{(i)}t_{I,0}^{(i-1)} - (t_{I,0}^{(i-1)})^2 \tag{15}$$

$$t_{P,n}^{(i)}(t_{P,n}^{(i)})^* \geq 2\Re\left\{t_{P,n}^{(i)}(t_{P,n}^{(i-1)})^*\right\} - t_{P,n}^{(i-1)}(t_{P,n}^{(i-1)})^* \tag{16}$$

$$\begin{aligned} t_{I,0}^{(i)}t_{P,0}^{(i)} &= \frac{1}{4}(t_{I,0}^{(i)} + t_{P,0}^{(i)})^2 - \frac{1}{4}(t_{I,0}^{(i)} - t_{P,0}^{(i)})^2 \\ &\geq \frac{1}{2}(t_{I,0}^{(i)} + t_{P,0}^{(i)})(t_{I,0}^{(i-1)} + t_{P,0}^{(i-1)}) \\ &\quad - \frac{1}{4}(t_{I,0}^{(i-1)} + t_{P,0}^{(i-1)})^2 - \frac{1}{4}(t_{I,0}^{(i)} - t_{P,0}^{(i)})^2 \end{aligned} \tag{17}$$

Frequency-flat IRS (4)

Hence, problem 9 is transformed to

$$\max_{\mathbf{\Phi}} \quad \tilde{z}(\mathbf{\Phi}) \tag{18a}$$

$$\text{s.t.} \quad \sum_n \log_2 \left(1 + \frac{(1-\rho)|w_{I,n}|^2 \mathrm{Tr}(\boldsymbol{R}_n \mathbf{\Phi})}{\sigma_n^2}\right) \geq \bar{R}, \tag{18b}$$

$$\mathbf{\Phi}_{l,l} = 1, \quad l = 1, \ldots, L+1, \tag{18c}$$

$$\mathbf{\Phi} \succeq 0, \tag{18d}$$

$$\mathrm{rank}(\mathbf{\Phi}) = 1 \tag{18e}$$

Waveform (1)

We optimize $\boldsymbol{w}_{I/P}$ with given IRS ϕ and splitting ratio ρ.

SDR: current expression

Introduce auxiliary variables

$$t'_{I/P,n} = \boldsymbol{w}_{I/P}^H \boldsymbol{H}_n^* \boldsymbol{w}_{I/P} = \mathrm{Tr}(\boldsymbol{H}_n^* \boldsymbol{W}_{I/P}) \tag{19}$$

Therefore, the current expression rewrites as

$$z(\boldsymbol{W}_{I/P}) = \frac{1}{2}\beta_2\rho(t'_{I,0}+t'_{P,0})+\frac{3}{8}\beta_4\rho^2\left(2(t'_{I,0})^2+\sum_{n=-N+1}^{N-1} t'_{P,n}(t'_{P,n})^*\right)+\frac{3}{2}\beta_4\rho^2 t'_{I,0}t'_{P,0} \tag{20}$$

Since 20 and 14 are in the same form, we use same Taylor approximation.

Waveform (2)

Hence, problem 9 is transformed to

$$
\begin{aligned}
\max_{\boldsymbol{W}_{I/P}} \quad & \tilde{z}(\boldsymbol{W}_I, \boldsymbol{W}_P) && \text{(21a)}\\
\text{s.t.} \quad & \sum_n \log_2\left(1 + \frac{(1-\rho) W_{I,n,n}|h_n|^2}{\sigma_n^2}\right) \geq \bar{R}, && \text{(21b)}\\
& \frac{1}{2}\left(\mathrm{Tr}(\boldsymbol{W}_I) + \mathrm{Tr}(\boldsymbol{W}_P)\right) \leq P, && \text{(21c)}\\
& \boldsymbol{W}_{I/P} \succeq 0, && \text{(21d)}\\
& \mathrm{rank}(\boldsymbol{W}_{I/P}) = 1 && \text{(21e)}
\end{aligned}
$$

Splitting ratio

We optimize ρ with given IRS ϕ and waveform $\boldsymbol{w}_{I/P}$.

$$\max_{\rho} \quad z(\rho) \tag{22a}$$

$$\text{s.t.} \quad \sum_n \log_2\left(1 + \frac{(1-\rho)|h_n w_n|^2}{\sigma_n^2}\right) \geq \bar{R}, \tag{22b}$$

$$0 \leq \rho \leq 1 \tag{22c}$$

Since $z(\rho)$ is a quadratic function that monotonically increases over $\rho \in [0, 1]$, we replace $z(\rho)$ with affine ρ and solve problem 22.

B. Clerckx, A. Costanzo, A. Georgiadis, and N. Borges Carvalho, "Toward 1G Mobile Power Networks: RF, Signal, and System Designs to Make Smart Objects Autonomous," *IEEE Microwave Magazine*, vol. 19, no. 6, pp. 69–82, 2018.

B. Clerckx, R. Zhang, R. Schober, D. W. K. Ng, D. I. Kim, and H. V. Poor, "Fundamentals of wireless information and power transfer: From RF energy harvester models to signal and system designs," *IEEE Journal on Selected Areas in Communications*, vol. 37, no. 1, pp. 4–33, 2019.

M. S. Trotter, J. D. Griffin, and G. D. Durgin, "Power-optimized waveforms for improving the range and reliability of RFID systems," *2009 IEEE International Conference on RFID, RFID 2009*, pp. 80–87, 2009.

Q. Wu and R. Zhang, "Intelligent Reflecting Surface Enhanced Wireless Network via Joint Active and Passive Beamforming," *IEEE Transactions on Wireless Communications*, vol. 18, no. 11, pp. 5394–5409, 2019.

——, "Towards Smart and Reconfigurable Environment: Intelligent Reflecting Surface Aided Wireless Network," *IEEE Communications Magazine*, vol. 58, no. 1, pp. 106–112, 2020.

——, "Weighted Sum Power Maximization for Intelligent Reflecting Surface Aided SWIPT," *IEEE Wireless Communications Letters*, pp. 1–6, 2019.

Y. Tang, G. Ma, H. Xie, J. Xu, and X. Han, "Joint Transmit and Reflective Beamforming Design for IRS-Assisted Multiuser MISO SWIPT Systems," 2019. [Online]. Available: http://arxiv.org/abs/1910.07156

C. Pan, H. Ren, K. Wang, M. Elkashlan, A. Nallanathan, J. Wang, and L. Hanzo, "Intelligent Reflecting Surface Aided MIMO Broadcasting for Simultaneous Wireless Information and Power Transfer," pp. 1–33, 2019. [Online]. Available: http://arxiv.org/abs/1908.04863

Q. Wu and R. Zhang, "Joint Active and Passive Beamforming Optimization for Intelligent Reflecting Surface Assisted SWIPT under QoS Constraints," pp. 1–30, 2019. [Online]. Available: http://arxiv.org/abs/1910.06220